Time Dependent Density Functional Theory Modeling of Specific Rotation and Optical Rotatory Dispersion of the Aromatic Amino Acids in Solution

Matthew D. Kundrat and Jochen Autschbach*

Department of Chemistry, 312 Natural Sciences Complex, The State University of New York at Buffalo, Buffalo, New York 14260-3000

Received: July 21, 2006; In Final Form: September 5, 2006

Time Dependent Density Functional Theory (TDDFT) along with the COnductor-like Screening MOdel (COSMO) has been applied to model the specific rotation at 589.3 nm and the optical rotatory dispersion (ORD) of the aromatic amino acids phenylalanine, tyrosine, histidine, and tryptophan. Solution structures at low, neutral, and high pH were determined. Both the anomalous dispersion absorbing (resonance) region and the lower energy (transparent) region of the ORD of the compounds were modeled. Linear response calculation of the specific rotation and ORD as well as Kramers−Kronig transformations of calculated circular dichroism spectra to model resonant ORD were compared with experimental data from the literature.

Introduction

All naturally occurring amino acids save the smallest, glycine, are chiral compounds. Each enantiomer of such a chiral compound can be distinguished from its mirror image by its specific rotation. Traditionally, specific rotation has been measured using the yellow sodium D-line of light, to which these amino acids are transparent. At this wavelength the specific rotation is expected to be strongly dependent on the lowest allowed electronic excitation. Historically, this transition has been identified as the n to π^* transition of the carboxylate functional group that is present in all of the free amino acids.[1]

The aromatic amino acids, phenylalanine, tyrosine, histidine, and tryptophan, differ from their aliphatic analogues in that in addition to this carboxylate chromophore they also possess an aromatic ring chromophore. The π to π^* transitions of the aromatic system have an additional effect on the chiroptical properties of these building blocks of proteins. Such transitions are of interest since they are primarily responsible for the circular dichroism (CD) features of proteins in the near-ultraviolet (UV).[2] There is a growing interest in using time-dependent density functional theory (TDDFT) to model this phenomenon. In fact, while this manuscript was in preparation Tanaka and co-workers published an article on using TDDFT to model the electronic and vibrational CD (ECD and VCD) of these very amino acids.[3]

That contemporary work by Tanaka et al. focused on modeling the configurations of the aromatic amino acids that are found in the random coil configuration of polypeptides, structures that are relevant to protein modeling. This current work focuses instead on the zwitterionic form of the molecules, and their various protonated and deprotonated forms in which these amino acids can be found in dilute aqueous solutions. Also while Tanaka et al. focused on modeling the absorptive chiroptical properties of these compounds, the ECD and VCD, this work instead models the dispersive properties, the specific rotation, and the optical rotatory dispersion (ORD) and how various chromophores affect these properties. This work constitutes a continuation of our previous work modeling specific rotation and ORD of the small aliphatic amino acids, alanine, proline, and serine, where the carboxylate chromophore was primarily responsible for the chiroptical response.[4] Here our calculations are extended to the larger, aromatic amino acids, in which two distinct chromophores contribute to the optical rotation.

To faithfully model chiroptical response properties one must first correctly determine the structures of the molecules being studied, and so this paper begins with a discussion of the optimized geometries of the amino acids. Some attention will be paid to the basis set effects on the relative energies of these geometries, and the relationship between basis set and the difficulty in correctly modeling the extent of intramolecular hydrogen bonding will be noted briefly. The computed mole fractions (Boltzmann populations) of the various conformers of some of these amino acids will be compared with experimentally derived Boltzmann populations from the literature. Next the specific rotations of select ionic states of these amino acids will be computed, and the results compared with experimental rotations. Particular attention will be paid to how the two different chromophores affect specific rotation, and how this varies depending on the conformation of the molecule. For some cases where the sign of the computed and measured specific rotation do not agree at 589 nm, it will be demonstrated how comparison of computed and measured optical rotatory dispersion curves would be a better method for assigning absolute configuration than comparison at 589 nm alone. Finally the anomalous optical rotatory dispersion of tyrosine in the near UV will be modeled in various protonation states via the Kramers−Kronig transformation of computed CD spectra and the results compared with experimental ORD.

Computational Methods

All data were computed with the Turbomole[5] quantum chemical software, version 5.7.1. The calculations were performed with B3-LYP[6] hybrid functional as implemented in the Turbomole code (note that this uses the VWN5 local correlation functional). Molecular geometries were optimized with the default doubly polarized valence triple-ζ (TZVPP) basis set from the Turbomole library; all energies reported herein were

* Corresponding author. E-mail: jochena@buffalo.edu.

10.1021/jp064636+ CCC: $33.50
Published on Web 11/08/2006

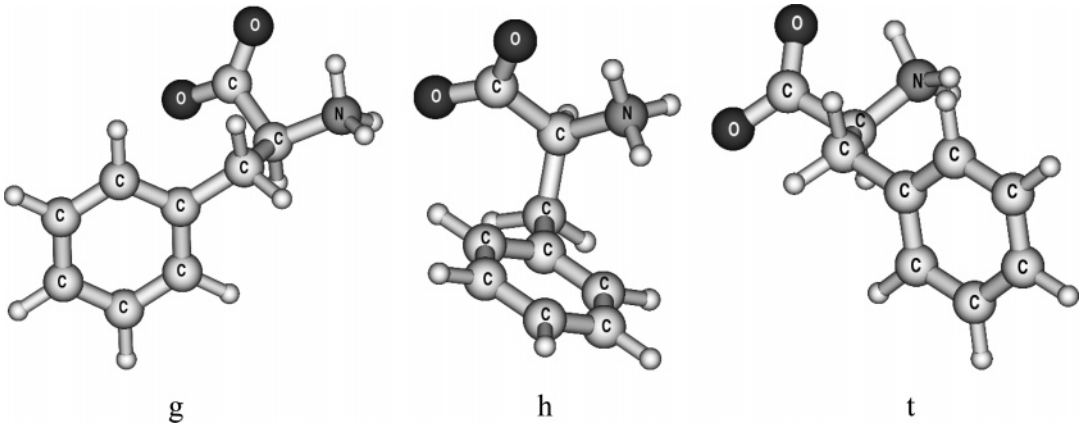

Figure 1. Optimized rotamers of the phenylalanine zwitterion.

computed with this basis. Response calculations were performed with the aug-cc-pVDZ set,[7] commonly used for the calculation of chiroptical properties. Where noted, corresponding response calculations were carried out using the TZVPP basis for comparison.

All optimizations and response calculations were performed with the COnductor-like Screening MOdel (COSMO)[8] of solvation applied to the ground state. Solvent model parameters were configured using the cosmoprep program of the Turbomole package. The dielectric constant of the solvent was set to 78; the Number of geometrical Segments Per Atom (NSPA) was set to 162; all other solvent parameters were left at program default values. Default optimized COSMO atomic radii were used.

Initial geometrical parameters were set with the Molden program.[9] All structures were confirmed local minima having no imaginary vibrational frequencies as calculated with the NumForce program. This numerical method of frequency computation was used since the analytical frequency module of the software was incompatible with the COSMO solvation method. In this paper the energy, "D", of a particular conformer is defined as the sum of the electronic energy, the solvation energy from the COSMO model, and the zero point energy calculated by NumForce. "ΔD" is defined as the energy of a particular conformer relative to the lowest energy conformation. Boltzmann factors were calculated based on this relative energy at the temperature of 293 K.

The Turbomole code presently does not support the use of Gauge Including Atomic Orbitals (GIAOs, also referred to as London Atomic Orbitals), so strictly speaking all calculated optical rotations are somewhat dependent on the gauge origin. Our origin is defined as the center of mass in each molecule. Such gauge origin dependence is known to diminish as the basis set size increases, and from a practical standpoint reasonably reliable results for small molecules are obtained by using the large augmented basis sets that are always needed to calculate reliable optical rotations.[10,11] Data in the literature support this conclusion.[12,13]

Except where otherwise noted, specific rotations were calculated at the wavelength of the sodium D line (589.3 nm). All specific rotations are reported in units of (deg·cm^3)/(g·dm). Optical Rotatory Dispersion (ORD) curves in the transparent region were computed similarly using a direct linear response method and plotted with values calculated at 10 nm intervals. Computed optical rotatory dispersion ORD curves in the absorbing region were obtained via a Kramers−Kronig transformation of computed electronic CD spectra using a numerical integration scheme recently recommended by Polavarapu.[14] Experimental ORD plots were scanned from their respective graphics in the literature, digitized using the WinDIG program,[15] and plotted alongside the calculated curves.

Results and Discussion

Structures of the Aromatic Amino Acids. Before the chiroptical properties of the aromatic amino acids can be modeled, it must first be acknowledged that these molecules possess a conformational freedom in solution at room temperature. The mole fractions of each conformer may be calculated based on the energy of each minimum using the Boltzmann equation. As such, the specific rotation measured from a solution of molecules is actually caused by a number of conformations, and the response observed is a weighted average of the effects of each conformer.

Free amino acids in solution can be found as three primary rotamers. These will be referred to herein as "g", "t", and "h", per the naming convention used by Martin et al.[16] The $C_{carboxyl}C_\alpha C_\beta C_\gamma$ dihedrals of the rotamers are approximately +60, 180, and −60 degrees, respectively. These three conformations are depicted in Figure 1, using the phenylalanine zwitterion as an example. In the g rotamer the aromatic ring is gauche to the carboxylate chromophore. In the t rotamer the phenyl group is trans to the acid functional group. In the h rotamer the aromatic ring is found adjacent to both the amino and acidic functional group, in a configuration that can be considered *hindered* from a steric viewpoint.

Each of the phenylalanine rotamers converged to an optimized geometry with the aromatic ring approximately perpendicular to the $C_\alpha-C_\beta$ bond. No corresponding local minima with the aromatic ring parallel to this bond could be found. Therefore for phenylalanine only three conformations were considered.

For tyrosine, histidine, and tryptophan more conformers are possible. These "subrotamers" are depicted in Figure 2. The tyrosine ring contains a hydroxyl functional group which can align itself in either of two directions, parallel to the ring. Histidine and tryptophan have asymmetric aromatic rings that can be found in two different configurations approximately perpendicular to the $C_\alpha-C_\beta$ bond. Tryptophan was unique in that additional conformations were found where the indole ring could converge to geometries nearly parallel to the $C_\alpha-C_\beta$ bond. However these conformers tended to be significantly higher in energy than the corresponding perpendicular conformations and were not considered further because of their negligible Boltzmann population. Therefore for each of these three amino acids two distinct subrotamers were modeled for a total of six possible conformers of each in the zwitterionic form.

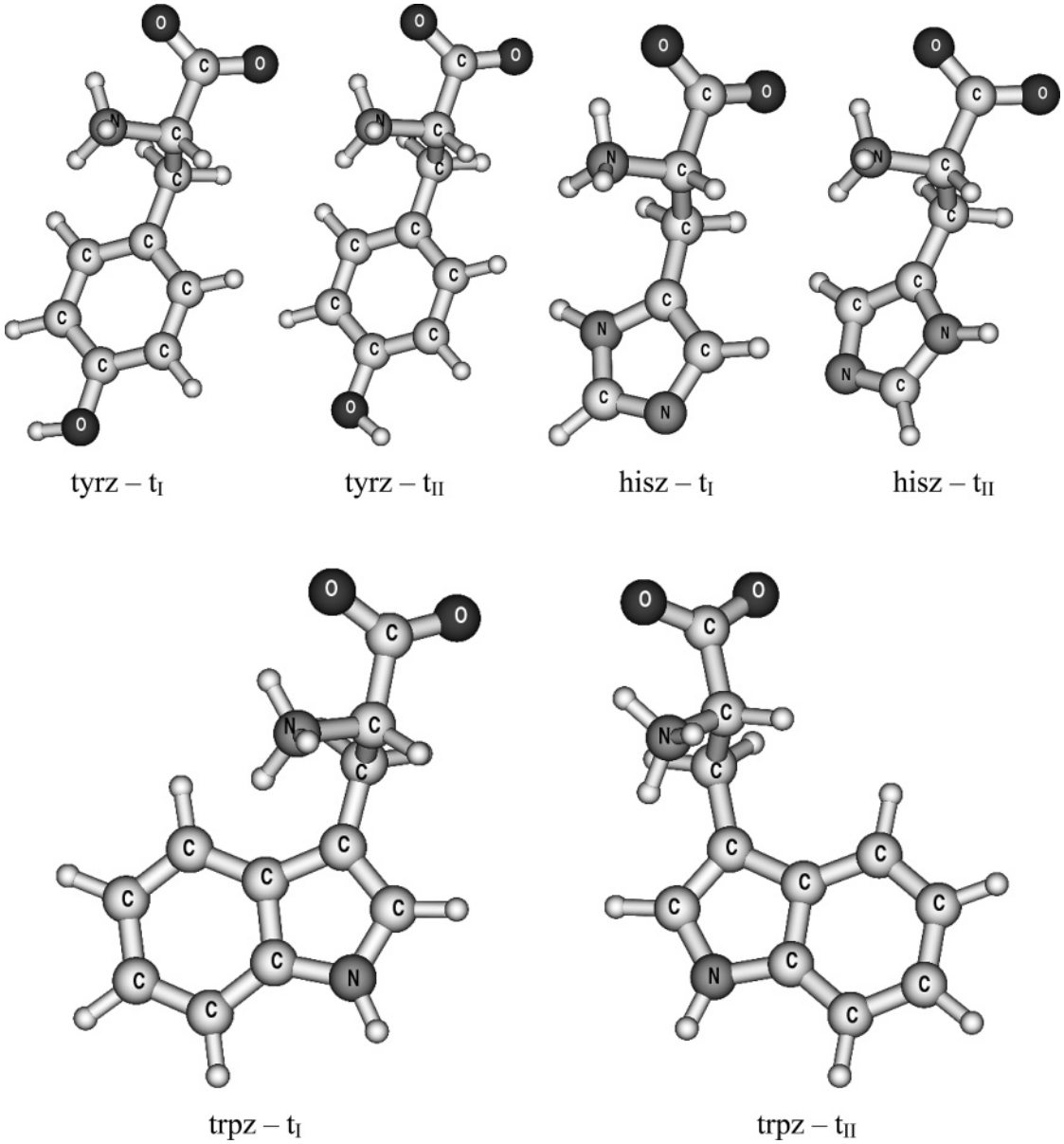

Figure 2. Selected optimized examples of the subrotamers of the tyrosine, histidine, and tryptophan zwitterions.

In addition to investigating the optical activity of these compounds near neutral pH, it is worthwhile to consider them at low pH, as a sizable amount of data are available on these molecules measured in strongly acidic conditions. Consequently the specific rotation of the protonated forms of these molecules also has been considered. Protonation of the COO^- functional group takes place preferentially on the oxygen more distant from the NH_3^+ group; this proton has a strong tendency to locate itself between the oxygen atoms. While other protonation locations are possible, an earlier study has indicated that they are high enough in energy relative to the ground state that these isomers are not significantly populated at room temperature.[4] Histidine is unique in this set of molecules in that it becomes doubly protonated at low pH. But since this second protonation can only occur at one position on the ring nitrogen atom, this does not lead to additional conformations, either. Therefore, just as with the zwitterions, six cationic (protonated) structures have been modeled for tyrosine, histidine, and tryptophan, and three structures were modeled for phenylalanine. An example of a doubly protonated molecule of histidine is depicted on the left side of Figure 3.

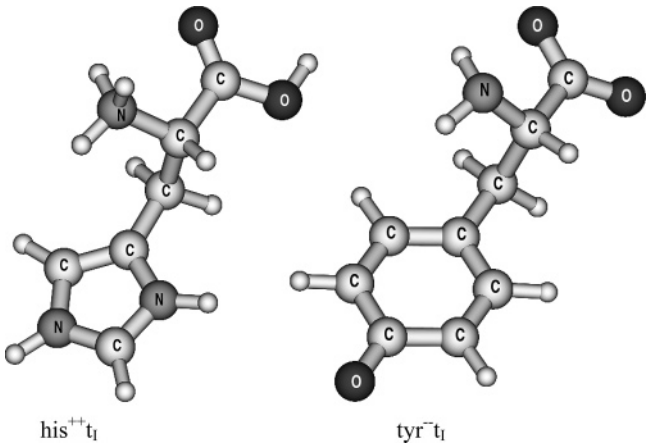

Figure 3. Select conformers of doubly protonated histidine and doubly deprotonated tyrosine.

Among the amino acids studied, tyrosine is unique in that it can become doubly deprotonated at high pH. Encouraged by the availability of experimental data on the optical activity of tyrosine at high pH (and the limited availability of experimental

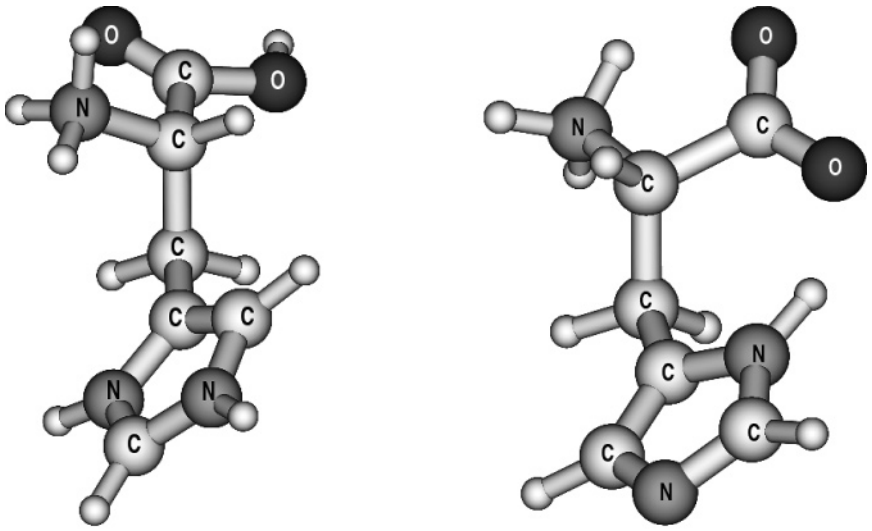

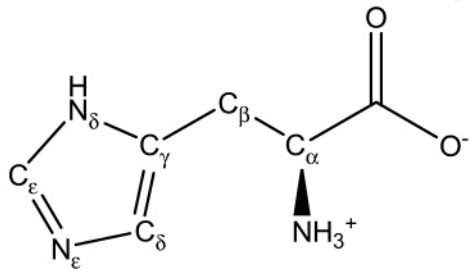

Figure 4. Top − the "parallel" conformers of histidine (left: dianion, right: zwitterion). The length of the hydrogen bond between the ring and carboxylate in the zwitterionic structure is 1.89 Å. Bottom − atom labeling for histidine.

data for this molecule near neutral pH) the specific rotation of dianionic (doubly deprotonated) tyrosine was also modeled. Compared to the zwitterion the conformational space of the tyrosine dianion simplifies as the phenolic hydrogen is removed but becomes more complex as any one of the three amino protons can be removed. All nine possible resulting conformers of the tyrosine dianion were considered, but the configuration depicted on the right side of Figure 3 was by far the lowest in energy and therefore dominates the analysis of the optical rotation. In this conformation the aromatic ring is trans to the carboxylate group, and the lone pair of the amino nitrogen is directed away from this ring.

For the sake of brevity not every optimized calculated structure has been depicted in this work. There are however two configurations not already shown that are worth noting. For differing reasons, two conformers of histidine converged to structures where the aromatic ring was more parallel than perpendicular to the $C_\alpha-C_\beta$ bond. Their structures are shown in Figure 4.

The misfit histidine dication conformer seems to result from repulsion between the NH_3^+ group and the imidazole ring. However ordinary steric repulsion alone is not sufficient to explain this geometry, since the analogous histidine zwitterion did optimize to a perpendicular conformation. The steric interaction between the previously mentioned groups remains virtually the same in the zwitterionic and dicationic forms of histidine. The charge on these groups is what changes upon protonation. In the dicationic form of this amino acid the amino group and the imidazole ring bear a significantly higher positive charge than they do in the zwitterionic form. An increased repulsion between positively charged functional groups could force the aromatic ring of the histidine dication away from its otherwise preferred perpendicular conformation into a more parallel one. The effect of this Coulomb repulsion on the geometry of the histidine molecule is shown in Table 1.

TABLE 1: Select Functional Group Charges and Geometric Data of "Trans" Rotamers of Histidine[a]

molecular charge	amine group charge	imidazole ring charge	amino N−δN distance (Å)	$C_\alpha-C_\beta-C_\gamma-C_\delta$ dihedral angle (deg)
−	−0.11	−0.16	3.341	−90
z	0.29	0.15	3.539	−77
+	0.69	0.88	3.623	−72
++	0.76	0.88	3.857	−52

[a] Charges reported represent the sum of the computed Mulliken charges for each moiety.

Coulomb repulsion is proportional to the product of the charges of two bodies and inversely proportional to their distance from one another. Based on the charge analysis the Coulomb repulsion should be the lowest in the anionic state and become progressively higher as the molecule is protonated. This repulsion may be relieved by the two groups moving farther away from each other, which happens in this case. The distance between the amino nitrogen and the aromatic ring atom closest to it, the nitrogen at the d position, progressively increases as the charge repulsion increases. As this part of the imidazole ring is repelled, the aromatic ring rotates, maintaining its rigid, planar form, and the dihedral angle about the $C_\beta-C_\gamma$ bond deviates from its ideal 90 degree configuration. This deviation grows progressively larger as the columbic repulsion increases, and at the doubly cationic protonation state the repulsion large enough that the aromatic ring is pushed beyond the 60 degree maximum that distinguishes "perpendicular" from "parallel" configurations, giving rise to the parallel configuration seen on the left of Figure 3.

The imidazole ring in the zwitterionic histidine conformation depicted on the *right* side of Figure 4 has also drifted away from the otherwise preferred perpendicular configuration. However here it is not repulsion but attraction between functional groups that causes this deviation. In this structure the ring has rotated to bring the NH group into close proximity to the COO^- group, allowing the two groups to hydrogen bond. The formation of this stabilizing intramolecular interaction causes the aromatic ring to deviate toward a parallel configuration in this instance.

This hydrogen bonding has been a potential source of error in the past, as the computational technique employed significantly overestimated the strength of intramolecular hydrogen bonding in zwitterions.[4] In those calculations the aug-cc-pVDZ basis was used, which includes diffuse functions. Diffuse functions have been regarded as important in modeling hydrogen bonding. While this basis was adequate for the geometry optimization and energy calculations of the small amino acids modeled in our earlier work, it proved problematic when dealing with the larger molecules in this current work. Here the TZVPP basis, which does not include diffuse functions, was used for geometry optimizations and energy calculations. It was chosen in part due to its established compatibility with the COSMO solvent model because the atomic radii were optimized for use with this basis which should therefore yield the most accurate solvation energies. The aug-cc-pVDZ basis was retained for the response calculations for which it is known to perform well. The use of different basis sets for optimizations and property calculations is well established in the field of computational chemistry, and efficiency regarding computing time by itself is enough to justify this practice. But there is another benefit from using a nondiffuse basis for these calculations.

Hydrogen bonding is an interaction between the orbitals of different atoms, be they on the same molecule (intramolecular) or between adjacent molecules (intermolecular). This bonding can take place over a significant distance, often 2 Å or more; this is why diffuse functions are needed to adequately describe it. In a system of hydrogen bonding molecules, such as an aqueous solution of an amino acid, an equilibrium exists between the tendency for a solute molecule to hydrogen bond with itself and its tendency to bond with solvent. When a continuum solvent model such as COSMO is used in lieu of explicit molecules to simulate solvation, this competition between inter- and intramolecular hydrogen bonding becomes biased toward the latter. With no explicit water molecules for the amino acid solute to hydrogen bond to, it has an overtendency to hydrogen bond with itself. Therefore, the amino acid conformations which include intramolecular hydrogen bonds become more favored energetically, and their computed Boltzmann populations become too high. This in turn can adversely alter the computed specific rotation of the solution, which depends in part on the computed populations of those conformers. We have investigated this issue in detail in a previous paper and concluded that the aug-cc-pVDZ + COSMO level indeed tends to overemphasize the internal hydrogen bonding in the zwitterionic amino acids.[4] Using a less-diffuse basis hinders hydrogen bonding somewhat. Since in the absence of explicit solvent molecules this (intramolecular) hydrogen bonding is too great, these two opposing errors partially compensate for each other yielding results that are somewhat closer to experiment. This first became apparent from calculations on the smallest amino acid, glycine. The previously mentioned earlier work with the COSMO/B3LYP/aug-cc-pVDZ method indicated that the zwitterionic form of glycine was favored over the neutral form by 4.6 kJ/mol. Here with the TZVPP basis it is calculated at 7.5 kJ/mol. Although this is only marginally closer to the experimental value of 30.4 kJ/mol,[17] it represents a significant relative change of the energy difference between the structures. We note in passing that switching to a basis that is not augmented with diffuse functions more than cuts in half the amount of "outlying charge" from the glycine zwitterion. This is the amount of electron density that escapes the COSMO model's outermost cavity and is a potential source of error.[18] Although it is far from being a perfect solvent model, the COSMO/B3LYP/TZVPP method has adequately modeled the fact that the zwitterionic form of the amino acids is more stable than the neutral form in aqueous solution.

TABLE 2: Computed Room Temperature Populations of Amino Acid Rotamers with Differing Basis Sets Compared to Experimental Data[h]

	computed population TZVPP	computed population aug-cc-pVDZ	experimentally derived population
		Phenylalanine Zwitterion	
g	0.03	0.03	0.24[a], 0.24[b]
h	0.21	0.19	0.27[a], 0.28[b]
t	0.76	0.78	0.50[a], 0.48[b]
		Phenylalanine Cation	
g^+	0.26	0.24	0.24[a], 0.28[b], 0.36[c], 0.32[f]
h^+	0.19	0.20	0.27[a], 0.26[b], 0.27[c], 0.26[f]
t^+	0.55	0.56	0.50[a], 0.46[b], 0.37[c], 0.42[f]
		Tyrosine Cation	
g^+	0.25	0.23	0.20[e]
h^+	0.20	0.20	0.40[e]
t^+	0.55	0.57	0.40[e]
		Tyrosine Dianion	
g^{--}	0.03	0.04	0.16[e]
h^{--}	0.03	0.02	0.38[e]
t^{--}	0.95	0.94	0.46[e]
		Tryptophan Zwitterion	
g	0.01	0.01	0.32[d], 0.26[f]
h	0.17	0.15	0.15[d], 0.23[f]
t	0.82	0.84	0.53[d], 0.51[f]
		Histidine Zwitterion	
g	0.44	0.63	0.18[g]
h	0.44	0.31	0.31[g]
t	0.11	0.07	0.51[g]
		Histidine Dication	
g^{++}	0.55	0.52	0.34[g]
h^{++}	0.11	0.13	0.28[g]
t^{++}	0.34	0.35	0.37[g]

[a] Kainosho and Ajisaka.[19] [b] Fujiwara et al.[20] [c] Hansen et al.[21] [d] Dezube et al.[22] [e] Juy et al.[23] [f] Reddy et al.[24] [g] Merrett et al.[25] [h] Computed populations for tyrosine, tryptophan, and histidine rotamers represent sums of the populations of two subrotamers per rotamer.

The basis set effects on the computationally derived mole fractions can be seen in Table 2. Here all geometries were computed with the TZVPP basis. The only variable that contributed to the differing Boltzmann populations between the two basis sets employed is the COSMO-corrected single point energy.

For the phenylalanine, tyrosine, and tryptophan molecules where intramolecular hydrogen bonding is not an issue the computed populations are nearly the same with the two basis sets. The agreement between these computed populations and those derived from experiment can be described as qualitatively correct. While the numerical agreement between experiment and theory is not perfect, both agree that for these three molecules the stericly favored t rotamers are more populated than their g and h counterparts at room temperature.

Consistent with our assumptions about controlling the intramolecular hydrogen bonding with the basis set, the results for histidine are different. Unlike the other aromatic amino acids, histidine shows a tendency to form intramolecular hydrogen bonds; the possibility for bonding exists between the carboxylate anion and the NH group at the d position of the aromatic ring. Such an interaction is favored in the g conformer depicted on the right side of Figure 4, where the two participating functional groups have been able to move into close proximity unhindered by the NH_3^+ group. Here the populations computed with the differing basis sets differ. While the population computed with the TZVPP basis overestimates the experimentally derived population of this hydrogen bonded conformer (at the expense of the t conformers in which the two groups are most distant and cannot bond), the diffuse aug-cc-pVDZ basis overestimates it even more. This is consistent with the theory that both methods overestimate the extent of intramolecular hydrogen bonding but the less-diffuse basis errors to a lesser extent. Therefore for the remainder of this work all Boltzmann populations reported will be computed from energies calculated with the TZVPP basis.

Computation of the Sodium D-Line Specific Rotation. Basis sets were also examined as they applied to the computed specific rotation. For nearly every conformation of every molecule investigated, the computed sign of the specific rotation was the same with the aug-cc-pVDZ and the TZVPP basis sets. The exceptions are the conformations that have specific rotations of too small a magnitude to be accurately calculated by this method. This should not be read to conclude that diffuse functions are not important for modeling specific rotation in general; oftentimes they are. But for this particular set of molecules the difference in chiroptical response between the two basis sets was not very significant.

The experimental and computed specific rotations of the four aromatic amino acids in select ionization states are shown in Table 3. At first glance, the agreement between theory and experiment appears somewhat disappointing, as the theory used herein yields a specific rotation that agrees in sign with experiment six out of nine times. But this is not unexpected when dealing with rotations that are so small in magnitude. Stephens and co-workers have shown the limitations of TDDFT for assigning absolute configuration of molecules with very small rotations.[26] When a small specific rotation value is the result of a delicate weighted average of several conformers having positive and negative optical rotations of large magnitude, then even a small error in computing the Boltzmann populations of these conformers could reverse the sign of the specific rotation. Furthermore, in cases where the measured specific rotation is exceedingly small, variations in laboratory conditions combined with the inherit limits of precision in the instrumentation can result in the sign of the experimentally measured rotation to itself be ambiguous, as was the case with the tryptophan cation discussed later in this paper. If it were the purpose of this work to assign configurations, using a shorter wavelength of light closer in energy to the lowest electronic excitation energies of the molecules in question would be advantageous because this would result in rotations much higher in magnitude and give a more accurate assignment. Here the sodium D-line light of 589.3 nm has been selected because most of the experimental data in the literature have been obtained at this convenient wavelength.

Of the possible sources of error, inaccuracy in the computed energy likely plays a large role. This energy is used to calculate the Boltzmann population of each conformer of a particular molecule. These factors are then multiplied by the specific rotation of each conformer, and the products are added to give the weighted average specific rotation that should be comparable to the experimentally observable value. As can be seen in Table 4, the specific rotations of some of these conformations are an order of magnitude larger than the average specific rotation that should be modeled. Since this relatively small weighted mean is produced from a number of conformers of relatively large specific rotations of differing signs, one can see how even a small error in a Boltzmann weighting factor can cause the computed average specific rotation to change sign.

Another important conclusion that the data lead to is that the method performs about equally regardless of the protonation state of the molecule being modeled. In an earlier work we have shown that TDDFT performed well in modeling the specific rotation of zwitterionic, cationic, and anionic amino acids in solution.[4] Here the specific rotation of an amino acid in its dicationic form, histidine, as well as an amino acid in its dianionic form, tyrosine, have been modeled with an equal margin of error. This is particularly gratifying in the case of the tyrosine dianion, due to the added difficulty of modeling electronic transitions in molecules with the more diffuse electronic structures found in anions. Different conclusions have been reached regarding whether TDDFT is adequate for modeling the optical rotation of similar anionic systems.[4,12] For this molecule the theory employed yields an average specific rotation of -32.0, which compares reasonably well with the experimental value of -13.2. The general overestimation of the magnitude of rotation is considered typical of TDDFT due in part to the known underestimation of excitation energies typically found for many organic molecules.[30] However, the correct modeling of the specific rotation of the molecules in this study depends not only on correctly modeling the excitation energies and rotatory strengths but also on computing the correct relative energies of the conformers and, in addition, a correct modeling of the solvation of the molecules being studied.

Contributions from Different Chromophores to the Specific Rotation. The primary purpose of this work has been not only to compare computed specific rotations of the aromatic amino acids with experiment but also to examine the interplay of the two different types of chromophores that are unique to the aromatics. The specific rotation of amino acids is generally thought to result from an n to π^* transition localized on the carboxylate chromophore. In aromatic compounds there also exists the possibility for a π to π^* transition involving the bonding and antibonding orbitals associated with the aromatic ring(s).

The effect of the carboxylate chromophore common to all the amino acids can be seen in the computed specific rotation of the various rotamers. The primary rotamers differ from one another by rotation about the $C_\alpha-C_\beta$ bond. The functional group that is responsible for perturbing the symmetry about the carboxylate group, in this case an aromatic ring, may be found in three orientations illustrated in Figure 1. For the g rotamers where the perturbing functional group is gauche to the carboxylate group on its stericly unhindered side the specific rotations are predominately positive. Conversely for the h rotamers when the perturbing group is on the opposite gauche side of the carboxylate group, the side that is stericly hindered by the ammonium group, the specific rotation is predominately negative. For the t rotamers where the perturbing group is trans to the carboxylate chromophore and most distant from it, the specific rotation is on the whole neither predominately negative nor positive when all the t conformations of all the molecules studied are considered. However the specific rotations of the t

TABLE 3: Computed and Experimental Data for the Specific Rotation of the Aromatic Amino Acids in Select Ionization States[c]

conformer	ΔD (kJ/mol)	Boltzmann factor	aug-cc-pVDZ specific rotation	aug-cc-pVDZ Boltzmann factor x specific rotation	TZVPP specific rotation	TZVPP Boltzmann factor x specific rotation	experimental specific rotation
			Phenylalanine Zwitterion				
t	0.0	0.76	6.7	5.1	18.2	13.8	
h	3.0	0.21	−150.9	−32.4	−120.6	−25.9	
g	7.6	0.03	162.4	5.0	142.8	4.4	
	average specific rotation			−22.3		−7.7	−35.1
			Phenylalanine Cation				
t^+	0.0	0.55	25.8	14.1	18.0	9.8	
g^+	1.8	0.26	221.8	58.1	210.4	55.1	
h^+	2.5	0.19	−69.1	−13.2	−66.7	−12.7	
	average specific rotation			59.0		52.2	−7.4[a]
			Tyrosine Zwitterion				
t_I	0.0	0.34	9.2	3.1	20.6	7.0	
t_{II}	0.2	0.31	−7.1	−2.2	4.1	1.3	
h_I	1.8	0.16	−132.9	−21.6	−104.5	−17.0	
h_{II}	3.3	0.09	−147.2	−12.5	−120.9	−10.3	
g_I	4.5	0.05	169.0	8.7	150.1	7.7	
g_{II}	4.7	0.05	167.7	8.0	145.3	6.9	
	average specific rotation			−16.5		−4.3	−10.0 to −12.3[b]
			Tyrosine Cation				
t_I^+	0.0	0.34	−12.2	−4.1	−15.0	−5.1	
t_{II}^+	1.1	0.21	−3.6	−0.8	−8.4	−1.8	
g_I^+	2.2	0.14	237.8	32.7	226.1	31.1	
h_I^+	2.4	0.12	−57.4	−7.0	−55.4	−6.8	
g_{II}^+	2.7	0.11	229.9	25.6	218.2	24.3	
h_{II}^+	3.6	0.08	−71.4	−5.4	−71.8	−5.5	
	average specific rotation			41.0		36.3	−10.6
			Tyrosine Dianion				
t_I^{--}	0.0	0.82	−36.3	−29.6	−25.5	−20.8	
t_{II}^{--}	5.8	0.07	−100.8	−7.3	−72.0	−5.2	
t_{III}^{--}	6.3	0.06	55.8	3.2	7.9	0.5	
h_I^{--}	9.4	0.02	−64.4	−1.0	−75.6	−1.2	
g_I^{--}	9.9	0.01	145.8	1.9	97.9	1.3	
g_{II}^{--}	9.9	0.01	101.8	1.3	72.1	0.9	
h_{II}^{--}	10.6	0.01	−60.3	−0.6	−25.7	−0.2	
g_{III}^{--}	14.4	<0.01	116.8	0.2	68.6	0.1	
h_{III}^{--}	15.2	<0.01	−71.8	−0.1	−38.0	−0.1	
	average specific rotation			−32.0		−24.8	−13.2
			Histidine Zwitterion				
g_I	0.0	0.44	115.5	51.1	108.3	47.9	
h_I	0.0	0.43	−196.6	−85.1	−147.3	−63.8	
t_I	3.4	0.11	−51.4	−5.4	−54.3	−5.7	
t_{II}	9.2	0.01	−72.6	−0.7	−42.1	−0.4	
h_{II}	9.7	0.01	−67.7	−0.5	−63.4	−0.5	
g_{II}	12.4	<0.01	213.4	0.5	196.9	0.5	
	average specific rotation			−40.2		−22.0	−38.95
			Histidine Dication				
g_I^{2+}	0.0	0.28	120.3	33.9	117.5	33.1	
g_{II}^{2+}	0.1	0.27	153.7	41.2	143.4	38.5	
t_I^{2+}	0.3	0.25	22.0	5.5	8.4	2.1	
t_{II}^{2+}	2.8	0.09	−73.8	−6.5	−76.9	−6.8	
h_I^{2+}	3.0	0.08	−74.9	−6.1	−67.1	−5.5	
h_{II}^{2+}	5.2	0.03	1.1	0.0	−8.8	−0.3	
	average specific rotation			67.9		61.1	13.34
			Tryptophan Zwitterion				
t_I	0.0	0.76	−22.0	−16.8	−30.6	−23.3	
h_I	4.2	0.13	8.8	1.2	14.2	1.9	
t_{II}	6.5	0.05	101.8	5.0	123.6	6.1	
h_{II}	6.8	0.04	−318.5	−14.3	−294.5	−13.2	
g_I	10.4	0.01	260.1	2.5	226.3	2.2	
g_{II}	15.0	<0.01	−46.3	−0.1	−48.2	−0.9	
	average specific rotation			−22.5		−27.4	−31.5
			Tryptophan Cation				
t_I^+	0.0	0.74	−73.0	−54.1	−82.6	−61.2	
h_I^+	5.3	0.08	89.6	7.2	84.0	6.8	
g_I^+	5.6	0.07	395.4	28.3	367.4	26.3	
g_{II}^+	7.0	0.04	−7.1	−0.3	−5.9	−0.2	
t_{II}^+	7.2	0.04	67.5	2.4	73.1	2.6	
h_{II}^+	7.5	0.03	−209.3	−6.5	−215.0	−6.7	
	average specific rotation			−22.9		−32.4	2.4

[a] Experimental data for phenylalanine cation from the work of Greenstein and Winitz.[28] [b] Experimental data for tyrosine zwitterion from World Wide Web.[29] [c] All specific rotation values are in (deg·cm^3)/(g·dm). Experimental data are from the *Merck Index*[27] except where otherwise noted.

rotamers are generally smaller in magnitude than their g and h counterparts. This is consistent with the idea that when the perturbing group is most distant from the perturbed chromophore, the perturbation of the symmetry of the chromophore is less significant, resulting in a smaller specific rotation.

For tyrosine, histidine, and tryptophan two subrotamers per rotamer can also be considered. These differ from one another by a rotation of approximately 180 degrees about the $C_\beta-C_\gamma$ bond and are designated simply as "I" and "II", with the former being lower in energy. No differing subrotamers of phenylalanine were found due to the symmetry of the phenyl ring.

For tryptophan in particular, a consistent difference in the specific rotation of pairs of subrotamers is observed. In all cases investigated, 3 pairs of zwitterionic geometries and 3 pairs of cationic geometries, each pair of subrotamers was found to have specific rotations of opposite sign. Here it is the $C_\beta-C_\gamma$ dihedral angle and not the $C_\alpha-C_\beta$ angle that is most important for determining the specific rotation of the conformer. In other words for tryptophan the orientation of the rest of the molecule with respect to the carboxylate chromophore has less of an effect on the specific rotation that the orientation of the rest of the molecule with respect to the indole chromophore. All conformations in which the rest of the tryptophan molecule is oriented on one side of the plane of the indole ring have a positive specific rotation, and all those in which the perturbation is on the opposite face have a negative specific rotation. This is the chiroptical response to be expected from an indole chromophore, which itself has C_s symmetry that can be perturbed to give either a positive or negative response depending on which side of the symmetry plane the perturbing atoms are oriented, in agreement with the well-known concept of sector rules.[31] The conclusion regarding the specific rotation of tryptophan is that the aromatic chromophore is primarily responsible for the observed specific rotation, and the carboxylate chromophore has a secondary effect. This is consistent with experimental[32] and theoretical[3] data which show significant CD excitations associated with the indole chromophore at energies lower than 250 nm. CD transitions that are largest in magnitude and closest to the energy where specific rotation is measured should have the greatest effect on its sign and magnitude, which is easily rationalized by the form of the denominator in the sum-over-states expression of optical rotation. The equation reads

$$[\alpha]_\omega = k\cdot\omega^2\cdot\sum_j \frac{R_j}{\omega_j^2 - \omega^2} \qquad (1)$$

where k is a constant, ω is the frequency, ω_j is an excitation frequency, and R_j is the corresponding rotatory strength for excitation number j. The sum formally runs over the complete set of excitations of the molecule.

Histidine like tryptophan contains an aromatic ring chromophore. This imidazole ring would belong to the C_{2v} point group were it not for the fact that the selective protonation of the nitrogen at the d position and the attachment of the rest of the molecule to the ring at a position that does not straddle the two nitrogen atoms reduce the site symmetry to C_s, which is then further perturbed to a chiral point group by the rest of the molecule. As with tryptophan, rotation about the $C_\beta-C_\gamma$ bond can have a significant effect on the specific rotation. But unlike with tryptophan the specific rotations of the pairs of subrotamers for histidine do not always have opposing signs. The specific rotation depends less on the $C_\beta-C_\gamma$ angle than on the $C_\alpha-C_\beta$ angle. The arguably higher symmetry of the imidazole ring compared to the indole ring might partially explain this difference. But an explanation for which there is observable physical evidence is that the energy for the lowest electronic transition for the imidazole ring is higher than that of the indole, as the first CD excitation for histidine is not observable until around 220 nm.[32] The first excitation energy of an imidazole ring is expected to be higher in energy than that of an indole ring since the imidazole has fewer π electrons and fewer atoms over which they are conjugated. Assuming similar magnitudes of the rotatory strengths, since the first π to π^* CD excitation occurs at a higher energy in histidine than in tryptophan, the histidine aromatic chromophore should have less of a dominating effect on the measured specific rotation, according to eq 1. Our computations indicate that in histidine both the aromatic and the carboxylate chromophores have significant effects on this optical activity.

For the tyrosine cation, different pairs of subrotamers do not yield significantly different specific rotations. The pairs of subrotamers of tyrosine only differ in the position of the phenolic hydrogen, which always orients itself in one of two positions in the plane of the aromatic ring. For the tyrosine dianion, this proton is removed and rotation of 180 degrees about the $C_\beta-C_\gamma$ bond yields degenerate structures. The dihedral angle about the $C_\alpha-C_\beta$ bond appears the most important for the tyrosine conformations studied, with the g rotamers always having a positive specific rotation, the h rotamers having a negative rotation, and the t rotamers showing neither tendency.

For phenylalanine, the effect of the phenyl chromophore on specific rotation cannot be modeled with the method used in this work. The six-membered aromatic ring in phenylalanine when unperturbed has D_{6h} symmetry, meaning that the lowest electronic excitation is symmetry forbidden. Experimentally vibronic coupling allows this weak transition to be observed in both ORD[33] and CD,[3] where the vibronic fine structure is clearly visible. But since vibronic coupling is not included in the method for computing specific rotation, the effects of the electronic transition in the aromatic chromophore cannot be analyzed. Such effects can be modeled, in principle, in a relatively straightforward manner in the CD[34] but would require excessive computational resources.

Computation of the Optical Rotatory Dispersion in the Near UV. To make an assignment of absolute configuration of a molecule, measurement and modeling of the specific rotation at 589.3 nm may be a convenient choice, but it is not the most accurate method. To make a comparison at higher frequencies where specific rotation is larger would likely add improvement, particularly in situations where differing conformations of a molecule have specific rotations of opposing signs at long wavelengths but agree in sign at shorter wavelengths closer to an excitation. For example, the computational method used thus far modeled the wrong sign for the specific rotation of the phenylalanine and tyrosine cations, but if the wavelength of 300 nm is used, which is close to but still lower than the first excitation energy of these molecules, then the experiment and the theory yield rotations that agree in sign. At this wavelength the specific rotation of protonated phenylalanine and tyrosine were measured as +91 and +132 (deg cm^3)/(g dm) and calculated to be +658 and +866 (deg cm^3)/(g dm), respectively. The overestimation of the magnitude of the rotation may to some extent be the result of using a method that does not include damping for excited states;[35] the exaggeration becomes more severe as the wavelength used is closer to an excitation energy, where the computed specific rotation would yield a singularity.

Comparing measured and modeled specific rotation at a single frequency can sometimes be useful in assigning absolute

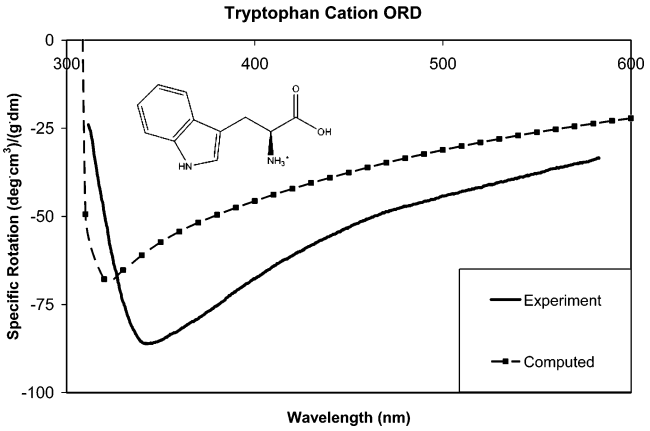

Figure 5. Computed and experimentally measured ORD of protonated tryptophan. Computed data points represent Boltzmann averages of optical rotations from six conformers. Experiential data are from the work of Djerassi.[37]

configuration. But to make this comparison over a large range of wavelengths, by computing an ORD curve and comparing it to experiment, would be the preferred method.[36] Transparent-region ORD curves are available in the literature for all of the molecules for which our theory does not model the correct sign of the sodium line specific rotation.[37] Of these the one for tryptophan is the most interesting due to its distinctive feature near 340 nm, so it is chosen here as a representative example.

The comparison of the ORD of tryptophan between 300 and 600 nm is depicted in Figure 5. The overall agreement between theory and experiment is quite good; the characteristic shape of the curve has been faithfully reproduced. Interestingly, *these* experimental data appear to agree with our calculations which indicate that the tryptophan cation has a rather large negative specific rotation near 589 nm. In fact, we found a number of sources in the literature that indicated that solutions of tryptophan in hydrochloric acid are dextrorotatory[27,28] and some that indicated that it is levorotatory[37,38] at this wavelength. This serves to further emphasize the point that comparing computed and measured specific rotation at a single wavelength is not the preferred method for assigning absolute configuration. Matching the shape of an ORD curve, as has been done in Figure 5, provides a far more reliable means for matching chiroptical response to structure.

The ORD that was measured and modeled in Figure 5 covers only wavelengths longer than the first excitation wavelength of the molecule. Based on their CD spectra both tyrosine and tryptophan are expected to have anomalous ORD features in the 225−300 nm region that should also be readily measurable. In fact near-UV region dispersion curves of tyrosine at a variety of pH conditions are available in the literature.[39,40] As these conditions correspond to some of the protonation states of tyrosine that were already modeled here, we have considered the ORD for this molecule as well.

The ORD of tryptophan in Figure 5 was successfully modeled by carrying out multiple linear response calculations. This covered only a region of wavelengths to which the molecule is transparent, so the lifetime broadening of the excited states was not of major concern. But when one calculates anomolous ORD with a program that does not include any damping in the linear response calculations, such as the one used in this work, singularities occur at all of the excitation wavelengths. Graphics depicting these effects on computed ORD curves can be found in the literature.[35,41]

At present, a program to calculate by direct linear response resonant ORD with hybrid functionals and the COSMO solvent

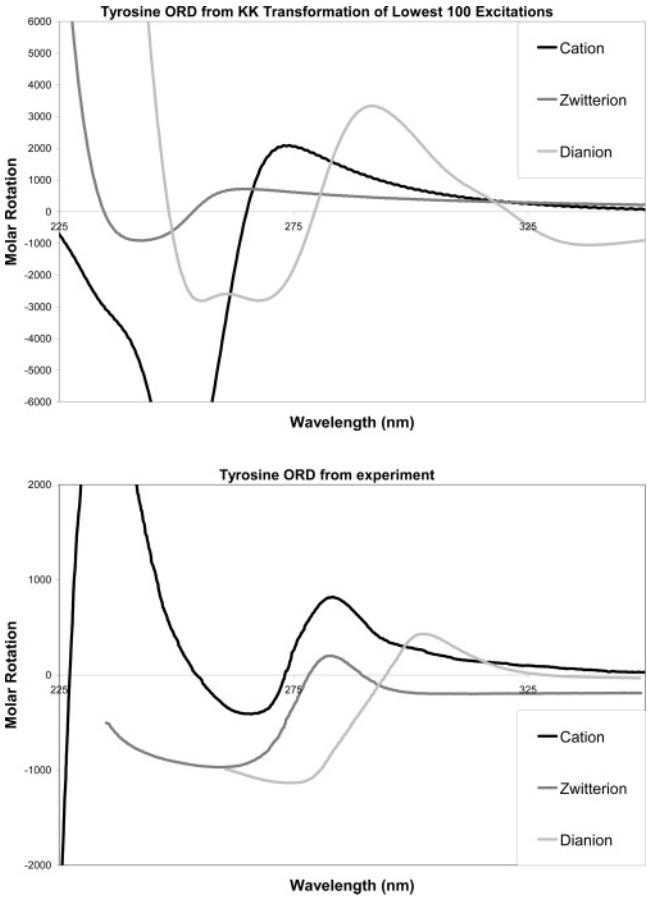

Figure 6. Computed (top) and experimental (bottom) ORD curves for tyrosine in various states of protonation. Experimental data for the cationic form are from Iizuka and Yang.[39] Experimental data for the zwitterionic and dianionic forms are from Hooker and Tanford.[40]

model is not available to us. The method used here to model resonant ORD is as follows: First the lowest 100 excitations of a CD spectrum for each conformation of each molecule studied were calculated. This is not meant to imply that 100 excitations are either necessary or sufficient to model the ORD in the region of interest; in fact we later found that truncating the series to five excitations did not significantly change the shape of the resultant ORD in the resonance region. The number 100 was chosen as an arbitrary cutoff to keep the computational time required to less than one processor week per calculation. There is no specific rule regarding how many excitations one should calculate for this method, and some truncation error is inevitable no matter where the cutoff is set.[14,42] Next the CD intensity was simulated using an empirical Lorentzian broadening with half-width at a half peak height of 0.19 eV. Then these CD spectra were transformed into ORD curves via a numerical Kramers−Kronig transformation as described in ref 42. Finally the resulting ORD curves of the individual conformers were Boltzmann averaged to produce the computed dispersion curve that is reported for each ionization state of tyrosine. The resulting plots are compared with experiment in Figure 6. This method was recently also used to successfully model the anomolous ORD of protonated proline through its first Cotton effect.[42]

As is shown in Figure 6, for all of the protonation states the theory correctly models the sign of the first Cotton effect. Furthermore, it correctly reproduces the experimentally observed trend that the first Cotton effect of the zwitterion occurs at a higher energy than that of the cation or dianion. The intensity of the effects is not correct, but this is largely affected by the

empirical broadening factor used. For the sake of simplicity a constant broadening factor was used, while in reality the broadening may be expected to increase with energy.

A limitation of this method is seen in the lower energy region away from the excitation. In this long wavelength area the ORD becomes increasingly dependent on a balance between low energy and the higher lying excitations. Since only a finite number of excitations can be included in the KK transformation, the truncation error becomes more of an issue in this low-energy area of the ORD where such excitations play a larger rule. This is why KK transformation of CD spectra is not the preferred method for computing ORD in the transparent region. As Polavarapu has stated earlier, direct linear response should instead be used to model ORD in the long wavelength region,[43] as was done in this work for the calculations at 589.3 nm and for the transparent region ORD of the tryptophan cation. KK transformations perform best for wavelengths that are in the vicinity of well separated electronic excitations, where, per the sum-over-states eq 1, the dispersion is dominated by these individual excitations. The purpose of using the Kramers−Kronig transformation here is to investigate the ORD in such an anomalous dispersion region. A comparison of the ORD in the vicinity of the first Cotton effect would be sufficient to match the chiroptical response with the correct enantiomeric structure. Just as others have used the KK transformation to model the anomolous ORD for several neutral organic molecules,[14] the method has proven useful here for investigating the ORD of the various protonation states of tyrosine as well. It appears that the modeling of resonant ORD by means of the KK transformations of a truncated CD spectrum well compliments linear response calculations of the ORD and specific rotation in the transparent region.

Conclusions

The specific rotation and optical rotatory dispersion of solutions of the aromatic amino acids in various protonation states have been modeled. The Boltzmann distribution of the low-energy conformations of the molecules was in qualitative agreement with experimentally derived distributions. The agreement was poorest for histidine due to difficulties with modeling of its intramolecular hydrogen bonding. Correct modeling of the specific rotation of the molecules at 589 nm proved a challenge since the rotations were relatively small in magnitude. However, some insight was gained about the effects of the different aromatic chromophores on this specific rotation. Comparison of computed and measured ORD over a broad range of wavelengths is clearly a more reliable method for assigning absolute configuration than comparison of specific rotation only at 589 nm. Kramers−Kronig transformation of computed CD spectra to ORD curves proved useful in modeling the sign and relative energy of the first Cotton effect for tyrosine in various protonation states.

Acknowledgment. We wish to thank Dr. Mykhalo Krykunov for his assistance with the Kramers−Kronig transformations. We also acknowledge the University at Buffalo Center for Computational Research (CCR) for maintenance of our computing resources. J.A. is grateful for financial support from the ACS Petroleum Research Fund and from the CAREER program of the National Science Foundation (CHE-0447321).

References and Notes

(1) Toome, V.; Weigele, M. *The Peptides* **1981**, *4*, 85.
(2) Rogers, D. M.; Hirst, J. D. *Biochemistry* **2004**, *43*, 11092.
(3) Tanaka, T.; Kodama, T. S.; Morita, H. E.; Ohno, T. *Chirality* **2006**, *18*, 652.
(4) Kundrat, M. D.; Autschbach, J. *J. Phys. Chem. A* **2006**, *110*, 4115.
(5) Ahlrichs, R.; Bar, M.; Haser, M.; Horn, H.; Kolmel, C. *Chem. Phys. Lett.* **1989**, *162*, 165.
(6) Becke, A. D. *J. Chem. Phys.* **1993**, *98*, 5648.
(7) Woon, D. E.; Dunning, T. H. *J. Chem. Phys.* **1994**, *100*, 2975.
(8) Schafer, A.; Klamt, A.; Sattel, D.; Lohrenz, J. C. W.; Eckert, F. *Phys. Chem. Chem. Phys.* **2000**, *2*, 2187.
(9) Schaftenaar, G. *Molden*, 4.4 ed.; Centre for Molecular and Biomolecular Informatics: 2005.
(10) Autschbach, J.; Patchkovskii, S.; Ziegler, T.; van Gisbergen, S. J. A.; Baerends, E. J. *J. Chem. Phys.* **2002**, *117*, 581.
(11) Lattanzi, A.; Viglione, R. G.; Scettri, A.; Zanasi, R. *J. Phys. Chem. A* **2004**, *108*, 10749.
(12) Pecul, M.; Ruud, K.; Rizzo, A.; Helgaker, T. *J. Phys. Chem. A* **2004**, *108*, 4269.
(13) Ruud, K.; Helgaker, T. *Chem. Phys. Lett.* **2002**, *352*, 533.
(14) Polavarapu, P. L. *J. Phys. Chem. A* **2005**, *109*, 7013.
(15) Lovy, D. *WinDIG*, 2.5 ed.; 2005.
(16) Martin, R. B.; Mathur, R. *J. Am. Chem. Soc.* **1965**, *87*, 1065.
(17) Wada, G.; Tamura, E.; Okina, M.; Nakamura, M. *Bull. Chem. Soc. Jpn.* **1982**, *55*, 3064.
(18) Klamt, A.; Jonas, V. *J. Chem. Phys.* **1996**, *105*, 9972.
(19) Kainosho, M.; Ajisaka, K. *J. Am. Chem. Soc.* **1975**, *97*, 5630.
(20) Fujiwara, S.; Ishizuka, H.; Fudano, S. *Chem. Lett.* **1974**, *11*, 1281.
(21) Hansen, P. E.; Feeney, J.; Roberts, G. C. K. *J. Magn. Reson.* **1975**, *17*, 249.
(22) Dezube, B.; Dobson, C. M.; Teague, C. E. *J. Chem. Soc., Perkin Trans. 2* **1981**, 730.
(23) Juy, M.; Hung, L. T.; Fermandjian, S. *Int. J. Pept. Protein Res.* **1982**, *20*, 298.
(24) Reddy, M. C.; Reddy, B. P. N.; Sridharan, K. R.; Ramakrishna, J. *Org. Magn. Reson.* **1984**, *22*, 464.
(25) Merrett, J. H.; Spurden, W. C.; Thomas, W. A.; Tong, B. P.; Whitcombe, I. W. A. *J. Chem. Soc., Perkin Trans. 1* **1988**, 61.
(26) Stephens, P. J.; McCann, D. M.; Cheeseman, J. R.; Frisch, M. J. *Chirality* **2005**, *17*, S52.
(27) *The Merck Index*, 12th ed.; Merck & Co., Inc.: Whitehouse Station, NJ, 1996.
(28) Greenstein, J. P.; Winitz, M. *Chemistry of the Amino Acids*; John Wiley & Sons: New York, 1961.
(29) ScienceLab.com; 2006; Vol. 2006.
(30) Bauernschmitt, R.; Ahlrichs, R. *Chem. Phys. Lett.* **1996**, *256*, 454.
(31) Berova, N.; Nakanishi, K.; Woody, R. W. *Circular Dichroism: Principles and Applications*, 2nd ed.; John Wiley & Sons: New York, 2000.
(32) Nishino, H.; Kosaka, A.; Hembury, G. A.; Matsushima, K.; Inoue, Y. *J. Chem. Soc., Perkin Trans. 2* **2002**, 582.
(33) Moscowitz, A.; Rosenberg, A.; Hansen, A. E. *J. Am. Chem. Soc.* **1965**, *87*, 1813.
(34) Neugebauer, J.; Baerends, E. J.; Nooijen, M.; Autschbach, J. *J. Chem. Phys.* **2005**, *122*, 7.
(35) Autschbach, J.; Jensen, L.; Schatz, G. C.; Tse, Y. C. E.; Krykunov, M. *J. Phys. Chem. A* **2006**, *110*, 2461.
(36) Giorgio, E.; Roje, M.; Tanaka, K.; Hamersak, Z.; Sunjic, V.; Nakanishi, K.; Rosini, C.; Berova, N. *J. Org. Chem.* **2005**, *70*, 6557.
(37) Djerassi, C. *Optical Rotatory Dispersion Applications to Organic Chemistry*; McGraw-Hill: New York, 1960.
(38) Patterson, J. W.; Brode, W. R. *Arch. Biochem.* **1963**, *2*, 247.
(39) Iizuka, E.; Yang, J. T. *Biochemistry* **1964**, *3*, 1519.
(40) Hooker, T. M., Jr.; Tanford, C. *J. Am. Chem. Soc.* **1964**, *86*, 4989.
(41) Giorgio, E.; Viglione, R. G.; Zanasi, R.; Rosini, C. *J. Am. Chem. Soc.* **2004**, *126*, 12968.
(42) Krykunov, M.; Kundrat, M. D.; Autschbach, J. *J. Chem. Phys.*, in press.
(43) Polavarapu, P. L. *Chirality* **2006**, *18*, 348.